

Preparation and physicochemical properties of zeolitic imidazolate framework-8 (ZIF-8)/rice husk derived graphene (GRHA) nanohybrid composites

N F T Arifin^{1,2}, N Yusof^{1,2*}, N A H M Nordin³, N I C Raimi⁴, J Jaafar^{1,2}, A F Ismail^{1,2}, F Aziz^{1,2} and W N W Salleh^{1,2}

¹Advanced Membrane Technology Research Centre (AMTEC), Universiti Teknologi Malaysia, 81310 Skudai, Johor Bahru, Malaysia

²School of Chemical and Energy Engineering (SCEE), Faculty of Engineering, Universiti Teknologi Malaysia, 81310 Skudai, Johor Bahru, Malaysia

³Department of Chemical Engineering, Universiti Teknologi PETRONAS, 32610 Bandar Seri Iskandar, Perak, Malaysia

⁴School of Mechanical Engineering (SME), Faculty of Engineering, Universiti Teknologi Malaysia, 81310 Skudai, Johor Bahru, Malaysia

*norhaniza@petroleum.utm.my

Abstract. This paper proposes an improve nanohybrid composites of Zeolitic Imidazolate Framework-8 (ZIF-8)/Rice husk Derived Graphene (GRHA). The main goal of this work is to prepare the nanohybrid composites with high surface area and enhanced porosity. The composite is prepared via aqueous room temperature method which is simple and fast. Based on Fourier transform Infrared (FTIR) and X-ray Diffraction (XRD) analysis, it shows that the produced ZIF-8 is in sodalite (SOD) structure while GRHA is in amorphous due to the presence of multilayer graphene. Raman analysis shows that the prepared GRHA has a high degree of graphitization. The BET specific surface area (BET_{SSA}) is found to increase up to three times higher ($1632.10 \text{ m}^2/\text{g}$) as compared to pristine GRHA ($518.11 \text{ m}^2/\text{g}$) and ZIF-8 ($687.32 \text{ m}^2/\text{g}$) respectively. Therefore, it is envisaged that this composite can be very useful for hydrogen storage.

1. Introduction

The demand of fossil fuel will keep increasing which can cause severe problem namely global warming. Hence, it is vital to overcome this issue by developing an alternative energies to the fossil fuels [1]. Hydrogen has been one of the best future energy as it can be used in electricity generation and alternative fuel for vehicles. Additionally, hydrogen is a clean energy as it does not emit CO_2 which reduces the environmental pollution [2]. Nevertheless, hydrogen storage has become the major issue that need to be resolved [3]. Currently, there are several ways that can be used to store hydrogen such as liquefaction [4], compression [5] and metal-hydride systems [6]. However, of all the aforementioned methods, adsorption via porous materials such as activated carbon nanofibers [7], porous carbons, zeolites and metal organic frameworks (MOFs) is favorable because of it fast kinetics, good cyclability and excellent adsorption capacity [1]. Currently, adsorption via metal organic frameworks (MOFs) shows a great promise for hydrogen storage [8]. In general, MOFs is composed of inorganic metal connectors and



organic linkers [9] which have high surface area and porosity [10], ordered crystalline structures as well as enhanced mechanical stability [9]. Zeolitic imidazolate frameworks-8 (ZIF-8) which is made up of zinc (Zn) metal and 2-methylimidazole (MIM) [11] has been studied extensively. Interestingly, ZIF-8 can be produced in deionized water at room temperature [12] which is fast and convenient [13].

It was said that, the properties of ZIF-8 can be further enhanced with the addition of graphene as the composites will have a better performance (hydrogen storage) [14] and higher surface area [15]. Unfortunately, the discovery of methods of producing was still under rapid progress. Even though chemical vapour deposition (CVD) has been an established method to produce graphene [16], but this method was complicated [17]. Currently, conversion of biomass material into graphene has received tremendous attention [18]. Rice husk, waste corn shell, egg shell and gelatin were some of the biomass precursors that can be used as a starting material to produce graphene [18,19]. Typically, potassium hydroxide (KOH) was used to activate biomass precursors as it will helps in the formation of pores [20] and producing a high purity graphene [21]. In general, rice husk contains 80 % of organic constituents such as lignin, cellulose and hemicellulose while the other 20 % is the inorganic silicon dioxide (SiO₂). Therefore, rice husk is one of the best precursors that can be used to synthesis rice husk derived graphene (GRHA) [22]. In this study, rice husk was activated with KOH to produce GRHA. Later, GRHA/ZIF-8 hybrid nanocomposites were synthesized through simple aqueous room temperature method to improve the physicochemical properties and the adsorption capacity of the material to store hydrogen gas.

2. Materials and Methodology

2.1. Materials

Rice husks were collected from Johor (Kilang Beras Jelapang Selatan Sdn. Bhd.). Zinc nitrate hexahydrate (Zn(NO₃)₂·6H₂O, 99 %), triethylamine (TEA) and 2-methylimidazole (2-MIM, 99 %) were purchased from Acros Organics while potassium hydroxide (KOH) was purchased from Quality Reagent Chemical (QReC).

2.2. Synthesis of GRHA

Rice husk was carbonized at 350 °C for 2 h to form rice husk ash (RHA). RHA (3 g) was mixed with KOH powder (15 g) and the mixture was annealed in a muffle furnace at 900 °C for 2 h. The GRHA was sonicated for 30 mins and washed with distilled water. Later, it was centrifuged at 3200 rpm for 10 mins for several times until neutral pH was obtained. Lastly, GRHA was dried in an oven at 80 °C overnight [23].

2.3. Preparation of ZIF-8 and GRHA/ZIF-8

ZIF-8 was prepared using the procedure as discussed by [12]. For the composites, metal solution was prepared by adding 2.95 g of Zn(NO₃)₂·6H₂O in 74 mL of deionized water and in a separate beaker, 0.2 g of GRHA was dispersed in 26 mL of deionized water. Both of the solution was mixed and sonicated for 30 min. Meanwhile, the ligand solution was prepared by adding, 6.5 g of 2-MIM and 20 mL of TEA in 100 mL of deionized water. The ligand solution was then added into the sonicated solution for 1 h under vigorous stirring. The solution mixture was allowed to be centrifuged and washed with deionized water. The product was then dried in an oven at 60 °C for 24 h and grounded into fine particles [24].

2.4. Characterization

In order to determine the functional groups attached on the samples, Fourier Transform Infrared (FTIR) was used. The IR spectra was collected after 32 scans in the 4000 – 500 cm⁻¹ regions. to determine the crystallinity of the samples, X-Ray Diffraction (XRD, Smart Lab, Rigaku) was used. Data was collected using Cu-K α radiation (1.54 nm) in the range of 2 θ from 5° to 50°. Brunauer-Emmet-Teller (BET) was used to analyze the surface area of GRHA, ZIF-8 and GRHA/ZIF-8. To analyze the degree of graphitization of GRHA, Raman spectroscopy (Horiba, Raman Xplora Plus) was used.

3. Results and discussions

3.1. FTIR analysis

GRHA shows a weak IR spectrum as it lacks functional groups (Refer figure 1 (a)). Therefore, GRHA only exhibits an obvious C-O vibration around 1080 cm^{-1} [25]. In contrast, ZIF-8 (Refer figure 1 (b)) confirms the presence of Zn-N and Zn-O bonds as it shows a vibrational peak at 657 cm^{-1} and 758 cm^{-1} respectively [26]. On the other hand, peaks at 1175 cm^{-1} and 1580 cm^{-1} indicate the stretching vibrations of C-N and C=N [27]. Interestingly, when GRHA is introduced into the nanocomposites, new stretching vibrations of C-H bond is formed (2930 cm^{-1}) (Refer figure 1 (c)) [28].

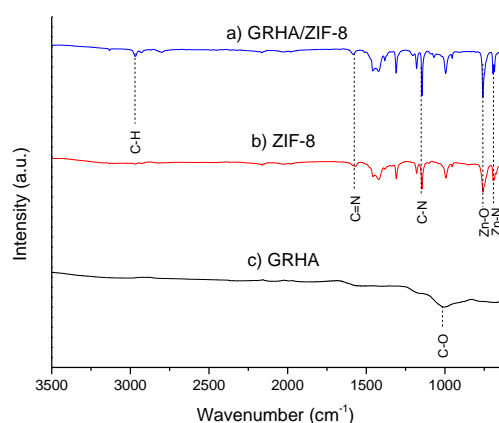


Figure 1. FTIR spectrum of (a) GRHA/ZIF-8 (b) ZIF-8 (c) GRHA.

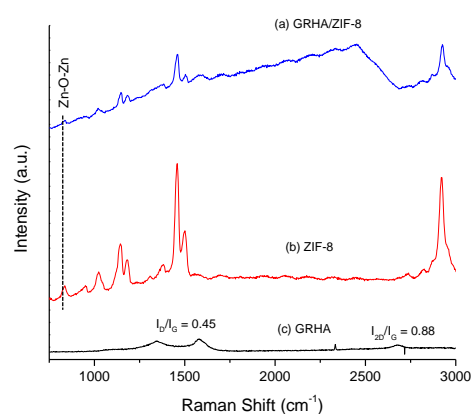


Figure 2. Raman shift of (a) GRHA/ZIF-8 (b) ZIF-8 (c) GRHA.

3.2. Raman analysis

I_D/I_G ratio of GRHA is calculated using Raman spectroscopy. This calculated value will indicate the degree of graphitization of GRHA [29]. In this study, it is found that the I_D/I_G ratio of GRHA (Refer figure 2 (c)) is 0.45 which suggests that the degree of graphitization of the sample is relatively high [30,31]. However, the intensity of D (1343 cm^{-1}), G (1577 cm^{-1}), and 2D (2675 cm^{-1}) peaks are quite low due to the multilayer structural defects [32]. For ZIF-8 (Refer figure 2 (b)), peaks at 390 cm^{-1} show the Zn-O-Zn vibrational bands and this peak can still be observed even after the addition of GRHA [33]. Therefore, it can be said that the addition of GRHA did not alter the Raman peak of GRHA/ZIF-8 (Refer figure 2 (a)).

3.3. Crystallinity study

Figure 3 (a) depicts that GRHA corresponds to few layers of graphene as it shows a broad peak at $2\theta = 26.62^\circ$ (002) [34]. In addition, the broad peaks indicate that the GRHA is in an amorphous state because of the presence of multilayer GRHA [27]. However, this result is similar as reported by [18]. On the other hand, XRD diffractogram of ZIF-8 (Refer figure 2 (c)) confirms the sodalite (SOD) structure of the samples because all peaks at (011), (002), (012), (022), (013), and (222) are observed [35]. Hence, a pure ZIF-8 has been successfully synthesized via aqueous room temperature method [36]. It can be seen from figure 3 (b) that the GRHA/ZIF-8 XRD diffractogram shows a higher peak intensity as compared to pristine ZIF-8 because the introduction of GRHA is able to remove guest molecules in the composites [12]. Nevertheless, the XRD diffractogram of both ZIF-8 and GRHA/ZIF-8 are almost similar. Therefore, it can be said that the addition of GRHA into the composites did not change the formation of ZIF-8 crystal structure [37].

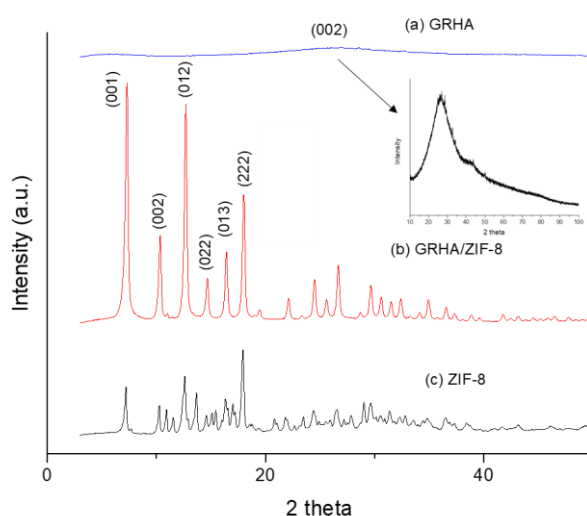


Figure 3. XRD spectrum of (a) GRHA (b) GRHA/ZIF-8 (c) ZIF-8.

3.4. Surface area analysis

In this study, the GRHA shows a BET specific surface area (BET_{SSA}) of $518.11 \text{ m}^2/\text{g}$ while ZIF-8 is $687.32 \text{ m}^2/\text{g}$ (Refer table 1). Interestingly, the nanocomposites of GRHA/ZIF-8 shows a significant change in the surface area where it shows BET_{SSA} up to $1632.10 \text{ m}^2/\text{g}$. The improvement of BET_{SSA} of GRHA/ZIF-8 is due to the combination of microporosity of ZIF-8 with mesoporosity of GRHA [24]. Moreover, the synergistic effect between GRHA and ZIF-8 also contributed to the increment of BET_{SSA} of the nanocomposites [38]. Besides that, the removal of guest molecules and formation of new pores after the addition GRHA also contributed to this phenomenon [39]. Previously, the highest BET_{SSA} obtained from GO/ZIF-8 is only $202 \text{ m}^2/\text{g}$ [24] and $917 \text{ m}^2/\text{g}$ [38]. This study produced GRHA/ZIF-8 nanocomposites with BET_{SSA} of $1632.1 \text{ m}^2/\text{g}$ which proves that our nanocomposites have an enhanced surface area.

Table 1. Specific surface area and porosity data.

Sample	BET_{SSA} (m^2/g)	Total pore volume (cm^3/g)	Micropore volume (cm^3/g)
GRHA/ZIF-8	1632.10	1.1694	0.8318
ZIF-8	687.32	0.3795	0.3036
GRHA	518.11	0.3346	0.2927

4. Conclusions

GRHA was synthesized through chemical activation using KOH whereas ZIF-8 and GRHA/ZIF-8 were formed through aqueous room temperature method. It is found that new C-H bond is formed which confirms the interaction between GRHA and ZIF-8. The prepared ZIF-8 shows a good crystallinity with sodalite (SOD) while the addition of GRHA into ZIF-8 did not alter the crystallinity of ZIF-8 which has been confirmed using XRD. GRHA exhibits amorphous structure because of the presence of multilayer graphene. However, Raman shift shows that GRHA has a relatively high degree of graphitization ($I_D/I_G = 0.45$). The introduction of GRHA into the composite greatly enhanced the BET_{SSA} which is $1632.10 \text{ m}^2/\text{g}$. Therefore, these findings suggest that GRHA/ZIF-8 can be a potential material for hydrogen storage since it has an enhanced physicochemical properties.

Acknowledgement

The authors would like to acknowledge the financial support from the Malaysian Ministry of Education and Universiti Teknologi Malaysia under UTM-Transdisciplinary Research Grant (Q.J130000.3551.06G07) and PRGS-ICC grant (R.J130000.7746.4J329). One of the authors N.F.T. Arifin would like to acknowledge Universiti Teknologi Malaysia for scholarship given under Zamalah scholarship.

References

- [1] Xia Y, Yang Z and Zhu Y 2013 *J. Mater. Chem. A* **1** 9365
- [2] Liew P Y, Kamaruddin M J, Ho W S Asli U A, Bong C P C, Hassim M H, Chemmangattuvalappil N G and Mah A X Y 2019 *Int. J. Hydrogen Energy* **44** 5661
- [3] Collins D J and Zhou H C 2007 *J. Mater. Chem.* **17** 3154
- [4] Cardella U, Decker L, Sundberg J and Klein, H 2017 *Int. J. Hydrogen Energy* **42**, 12339
- [5] Mazloomi K, and Gomes C 2012 *Renew. Sustain. Energy Rev.* **16** 3024.
- [6] Bellosta von C J, Ares J R, Barale J, and Baricco M 2019 *Int. J. Hydrogen Energy* **44** 7780
- [7] Che O F E, Yusof N, Hasbullah H and Jaafar J 2017 *J. Ind. Eng. Chem.* **51** 281
- [8] Yan Y, Da Silva I, Blake A J and Dailly A 2018 *Inorg. Chem.* **57** 12050
- [9] Zheng Y Y, Li C X, Ding X T and Yang Q 2017 *Chinese Chem. Lett.* **28**, 1473
- [10] Szczeńśniak B, Choma J and Jaroniec M 2018 *Appl. Surf. Sci.* **459** 760
- [11] Lee Y R, Jang M S, Cho H Y and Kwon H J 2015 *Chem. Eng. J.* **271** 276
- [12] Nordin N A H M, Ismail A F, Mustafa A and Goh P S 2014 *RSC Adv.* **4** 33292
- [13] Khan I U, Othman M H D, Jilani A and Ismail A F 2018 *Arab. J. Chem.* **8** 0
- [14] Pokhrel J, Bhorla N, Anastasiou S and Tsoufis T 2018 *Microporous Mesoporous Mater.* **267** 53
- [15] Szczeńśniak B, Choma J and Jaroniec M 2018 *J. Colloid Interface Sci.* **514** 801
- [16] Lee H C, Liu W W, Chai S P and Mohamed A R 2016 *Procedia Chem.* **19** 916
- [17] Seah C M, Chai S P and Mohamed A R 2014 *Carbon N. Y.* 2014 **70** 1
- [18] Purkait T, Singh G, Singh M, Kumar D and Dey R S, *Sci. Rep.* **7** 1
- [19] Chen F, Yang J, Bai T, Long B and Zhou X 2016 *J. Electroanal. Chem.* **768** 18
- [20] Ojha K, Kumar B and Ganguli A K 2017 *J. Chem. Sci.* **129** 397
- [21] Priyanka M and Saravanakumar M P 2017 *IOP Conf. Ser. Mater. Sci. Eng.* **263** 246
- [22] Sankar S, Lee H, Jung H and Kim A 2017 *New J. Chem.* **41** 13792
- [23] Muramatsu H, Kim, Y A, Yang K S and Cruz-Silva, R 2014 *Small* **10** 2766
- [24] Kim D, Kim D W, Hong W G and Coskun A 2016 *J. Mater. Chem. A* **4** 7710
- [25] Çiplak Z, Yildiz N and Çalimli, A 2015 *Fullerenes, Nanotub. Carbon Nanostructures* **23** 361
- [26] Wang J, Li Y, Lv Z and Xie Y 2019 *J. Colloid Interface Sci.* **542** 410
- [27] Jamil N, Othman N H, Alias N H and Shahrudin M Z 2019 *J. Solid State Chem.* **270** 419
- [28] Chen J, Liu K, Jiang M and Han J 2019 *Colloids Surfaces A Physicochem. Eng. Asp.* **568** 461
- [29] Zhipeng W, Hironori O, Shingo M and Josue O M 2015 *Carbon N. Y.* **94** 479
- [30] Cao Y, Wang K, Wang X and Gu Z 2016 *Electrochim. Acta* **212** 839
- [31] Jung S H, Myung Y, Kim B N and Kim I G 2018 *Sci. Rep.* **8** 1
- [32] Shams S S, Zhang L S, Hu R, Zhang R and Zhu J 2015 *Mater. Lett.* **161** 476
- [33] Kumar R, Jayaramulu K, Maji T K and Rao C N R 2013 *Chem. Commun.* **49** 4947
- [34] Gupta B, Kumar N, Panda K and Kanan V 2017 *Sci. Rep.* **7** 45030
- [35] Pokhrel J, Bhorla N, Anastasiou S and Tsoufis T 2018 *Microporous Mesoporous Mater.* **267** 53
- [36] Chen B, Wan C, Kang X and Chen M 2019 *Sep. Purif. Technol.* **223** 113
- [37] Tsoufis T, Tampaxis C, Spanopoulos I and Steriotis, T 2018 *Microporous Mesoporous Mater.* **262** 68
- [38] Thomas M, Illathvalappil R, Kurungot S and Nair, B.N 2016 *ACS Appl. Mater. Interfaces* **8** 29373
- [39] Md Nordin N A H, Racha S M, Matsuura T and Misdan N 2015 *RSC Adv.* **5** 43110